



## Original Article

## Effect of two way thermal hydraulic-fuel performance coupling on multicycle depletion

Awais Zahur <sup>a</sup>, Muhammad Rizwan Ali <sup>a</sup>, Deokjung Lee <sup>a,b,\*</sup><sup>a</sup> Department of Nuclear Engineering, Ulsan National Institute of Science and Technology, 50 UNIST-gil, Ulsan, 44919, Republic of Korea<sup>b</sup> Advanced Nuclear Technology and Services, 406-21 Jonga-ro, Jung-gu, Ulsan, 44429, Republic of Korea

## ARTICLE INFO

**Keywords:**  
 Multicycle depletion  
 CTF  
 FRAPCON  
 Multiphysics  
 External loose coupling

## ABSTRACT

A Multiphysics coupling framework, MPCORE, has been developed to analyze safety parameters using the best estimate codes. The framework contains neutron kinetics (NK), thermal hydraulics (TH), and fuel performance (FP) codes to analyze fuel burnup, radial power distribution, and coolant temperature ( $T_{bc}$ ). Shuffling and rotation capabilities have been verified on the Watts Bar reactor for three cycles. This study focuses on two coupling approaches for TH and FP modules. The one-way coupling approach involves coupling the FP code with the NK code, providing no data to the TH modules but getting  $T_{bc}$  as boundary condition from TH module. The two-way coupling approach exchanges information from FP to TH modules, so that the simplified heat conduction solver of the TH module is not used. The power profile in both approaches does not differ significantly, but there is an impact on coolant and cladding parameters. The one-way coupling approach tends to over-predict the cladding hydrogen concentration (CHC). This research highlights the difference between one-way and two-way coupling on critical boron concentration,  $T_{bc}$ , CHC, oxide surface temperature, and pellet centerline temperature. Overall, MPCORE framework with two-way coupling provides a more accurate and reliable analysis of safety parameters for nuclear reactors.

## 1. Introduction

Benchmark data from several operational nuclear plants have made it possible for computational codes to model and verify various parameters of interest with high accuracy [1,2]. For better comparison with the benchmark results, Multiphysics coupling analysis is required. Single physics codes often simplify the other physics phenomenon by taking conservative assumptions on their part. For instance, single physics neutron kinetics (NK) codes can determine the flux distribution, axial shape index, and burnup at the end of a cycle by using simple 1D thermal hydraulic (TH) codes and constant gap heat transfer coefficient. NK options include nodal diffusion codes [3–7], lattice physics transport codes [8,9], and Monte Carlo codes [10–13]. To improve accuracy, researchers have increasingly focused on Monte Carlo codes to reduce RMS errors for power and burnup during the cycle. TH codes can identify the maximum coolant temperature during normal operation of a nuclear power plant as well as departure from nucleate boiling ratio (DNBR). Thermal hydraulic codes range from three dimensional CFD codes, subchannel thermal hydraulic codes to simplified 1D TH codes. Fuel performance analysis, on the other hand, ensures that the enthalpy

and fuel centerline temperature are within permissible limits to avoid meltdown and to predict pellet clad mechanical interaction. FP codes can range from 3D to 1D codes assuming the dominant heat transfer process from all 3 dimensions to in single dimension respectively.

In actual, NK, TH, and FP phenomena are inherently dependent on each other. Fission cross-sections, burnable material absorption cross-sections, and moderator scattering cross-sections are all dependent on fuel and moderator temperatures. This temperature dependence necessitates the coupling of thermal hydraulics codes with neutronics options. Several efforts have been made to couple different physics codes for analysis. Loose external coupling using data exchange files has been implemented in MCNPX and COBRA subchannel codes for steady-state analysis [14]. For hot full power steady-state solutions in fuel assembly and full core, Monte Carlo code MC21 was coupled with subchannel TH code, CTF [15]. Depletion calculation of fuel assembly has also been performed by coupling Monte Carlo code SERPENT with subchannel TH code, Sub-ChanFlow, and FP code TRANSURANUS [11,16]. Transport codes have also been coupled with subchannel TH codes to perform fuel conduction, deformation, and cladding heat transfer [17–19]. Nodal codes with subchannel thermal hydraulic code were also coupled for

\* Corresponding author. Department of Nuclear Engineering, Ulsan National Institute of Science and Technology, 50 UNIST-gil, Ulsan, 44919, Republic of Korea.  
 E-mail address: [deokjung@unist.ac.kr](mailto:deokjung@unist.ac.kr) (D. Lee).

steady-state depletion and transient analysis [20].

Although fuel performance codes are not typically used in coupled analysis, they are often used to model burned fuels to check for PCMI and cladding stress [21]. FP codes not only model dynamic gap conductance, but also account for changes in thermal conductivity of fuel and cladding with burnup. Additionally, oxide layer formation on the clad surface can be modeled by FP codes. FP codes have also been used to predict accurate fuel cladding hydride precipitates that make cladding vulnerable to cracking. Experiments have also shown the importance of hydrogen concentration on burst parameters of zircaloy cladding [22]. In previously reported Tiamat coupling approach, CTF was used to give clad surface temperature to BISON for FP studies [23, 24].

The integration of neutronics, thermal hydraulics, and fuel performance codes through a coupling framework has a significant impact on the cladding hydrogen concentration (CHC) and coolant temperature profile during the depletion cycle of nuclear reactors. The MPCORE Multiphysics framework has already coupled the fuel performance module. This research focuses on comparing one-way and two-way coupling of the FP/TH module and their impact on safety parameters.

## 2. Computer codes description

### 2.1. Neutronics code RAST-K

The conventional two-step modeling approach is utilized for neutronics calculations. Lattice code, STREAM, is used to generate fuel assembly and reflector cross-sections, as well as group constants. For this research, the ENDF/B-VII.1 and JENDL-4.0 mixed cross-section library is employed in STREAM. Fuel material cross-sections at 540 K, 900 K, and 1500 K are used, while moderator materials cross-sections at 540 K, 565 K, and 590 K are employed. The boron concentration values used are 0.1, 650, 1300, and 2400 ppm. Cross-sections are generated for both control rod inserted and withdrawn cases for all assemblies. In total, 28 branch cases are created for the hot state with different combinations of temperatures and boron concentrations at burnup points ranging from 0 to 80 MWD/kg. STORA is used to link the group constants, number density, and form functions of all assemblies into one XS file.

The nodal code RAST-K is then used to solve the 3D diffusion equation for the flux and power distribution in the whole/quarter core. The Unified Nodal method, which includes pin power reconstruction, is implemented in RAST-K. To solve the Bateman equations for depletion calculations, RAST-K uses the Chebyshev rational approximation method [4]. The STREAM/RAST-K two-step code has already been validated for benchmark problems involving operational nuclear power plants [5,6]. The shuffling and rotation utility developed in RAST-K is employed to analyze multicycle depletion problems.

Spacer grid homogenization is generally used for nodal code solutions, but for the current analysis, heterogeneity is maintained by using different cross-sections for the spacer grid portion, with spacer grid smearing in coolant. The non-spacer grid portion uses cross-sections without zircaloy/Inconel smearing.

### 2.2. The thermal hydraulic code CTF

The CTF subchannel thermal hydraulic code is a thermal hydraulic code developed and maintained by Pennsylvania State University (PSU) and North Carolina State University (NCSU) [25]. It can perform thermal hydraulic studies that incorporate cross flow effects, and its parallelization framework allows for fast computation through MPI. The CTF coupling interface is designed to facilitate in-memory data exchange between CTF and external codes, which makes it easier to incorporate into larger models that include other physics modules.

CTF is a channel-centered code, whereas the neutronics and fuel performance modules are exchanging data on a rod basis. Therefore, rod-centered information is also utilized in CTF. For the calculation of

the film heat transfer coefficient, the Chen correlation is employed, and the W3 correlation is used for DNBR calculations. CTF utilizes its own heat conduction solver unless it is explicitly turned off.

In a one-way coupling of thermal hydraulics (TH) and fuel performance (FP) modules, CTF uses its own conduction solver and provides the coolant temperature as a boundary condition to FP. In CTF, the default conduction correlation, MATPRO-11, is utilized that does not incorporate the burnup term. Although CTF offers a burnup-dependent fuel conductivity correlation (modified NFI correlation), it remains unused in the current analysis due to the absence of a depletion solver. Consequently, the gap conductivity in CTF relies solely on power without considering any isotopic changes in the gap, leading to a constant gap conductivity while fuel conductivity decreases. In contrast, MATPRO-11 maintains the independence of both fuel and gap conductivity from burnup.

MATPRO-11 correlation (used by CTF) is given as:

$$K_{UO_2} = C \left\{ \max \left( \frac{2335}{464 + T_c}, 1.1038 \right) + 7.027 \cdot 10^{-3} \exp(1.867 \cdot 10^{-3} T_c) \right\}, \text{ where}$$

$$C = \frac{1 - \beta(1 - D)}{1 - 0.05\beta}, \text{ and}$$

$$\beta = 2.58 - (5.8 \cdot 10^{-4}) T_c$$
(2.1)

While modified NFI correlation (used by FRAPCON) is given as:

$$K_{95} = \frac{1}{A + a \cdot gad + BT + f(Bu) + (1 - 0.9 \exp(-0.04Bu))g(Bu)h(T)}$$

$$+ \frac{E}{T^2} \exp\left(-\frac{F}{T}\right)$$
(2.2)

Where,

K95 = thermal conductivity for 95% TD fuel (W/m-K)

T = temperature (K)

Bu = burnup (GWd/MTU)

f(Bu) = effect of fission products in crystal matrix (solution) = 0.00187. Bu

g(Bu) = effect of irradiation defects = 0.038. Bu<sup>0.28</sup>

h(T) = temperature dependence of annealing on irradiation defects = 1/(1 + 396e<sup>-Q/T</sup>)

Q = temperature dependence parameter ("Q/R") = 6380 K.

A = 0.0452 (m-K/W)

a = constant = 1.1599

gad = weight fraction of gadolinia.

B = 2.46E-4 (m-K/W/K)

E = 3.5E9 (W-K/m)

F = 16361 (K)

The burnup term is present in modified NFI correlation that is absent in MATPRO-11 correlation.

In a two-way coupling, the conduction option is turned off in CTF, and the oxide surface temperature obtained from FP module is set in CTF.

CTF can model a full core with a quarter symmetry option, which allows for a reduced number of modeled fuel assemblies, thus requiring fewer processors to run in parallel. Overall, the flexibility and versatility of the CTF code, along with its robust parallelization framework and coupling interface, make it a valuable tool for thermal hydraulic analysis in nuclear engineering applications.

### 2.3. The fuel performance code FRAPCON

In the coupling framework, the fuel performance code utilized is the Fuel Rod Analysis Programming Interface (FRAPI) [26], which allows

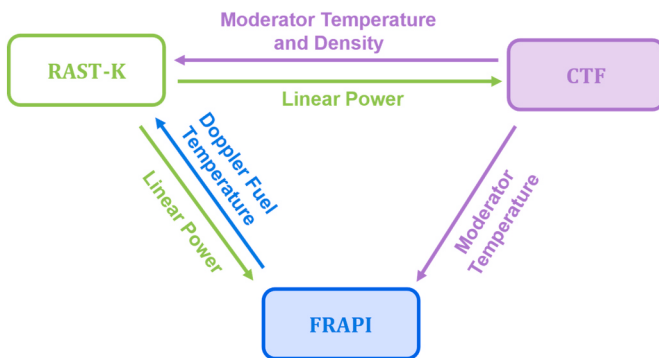


Fig. 1. One-way coupling between TH and FP modules.

for coupling between FRAPCON [27] and FRAPTRAN [28] for depletion and transient calculations respectively. FRAPI is equipped with important features such as writing and reading restart files at every burnup step. FRAPCON, a 1.5D fuel performance code developed by Pacific Northwest National Laboratory, is written in Fortran and offers several significant features such as dynamic gap heat conductance, predominantly radial heat conduction, and burnup dependent correlations of heat conduction.

FRAPCON includes a model for the oxide thermal barrier, which causes the oxide layer to grow with time. Initially, the clad outer surface temperature and oxide surface temperature are the same since there is no oxide layer. However, as the oxide layer grows due to burnup and coolant flow, the temperature difference between the clad outer and oxide layer widens. During the nuclear fuel cycle, fuel expansion, cladding creep, hoop stress, and fuel cracks may occur due to power transients. These models are developed in FRAPCON and used in industrial applications for fuel deformity and pellet clad mechanical interaction analysis. Additionally, IFBA rods used to control power peaking at the beginning of a cycle can be modeled with FRAPCON, as helium production due to IFBA coatings of ZrB<sub>2</sub> increases the rod internal pressure. The hydrogen pickup fraction from metal-water corrosion reaction, for Zircaloy-4, is kept constant at 0.15 and the CHC is affected by the temperature distribution.

MPCORE handles shuffling and rotation of fuel assemblies. Due to parallel implementation, the total number of rods are divided equally among all the processors. Depletion information between RAST-K and FRAPCON is not transferred since FRAPCON has its own depletion module.

### 3. Coupling code description

The external loose coupling framework, MPCORE developed by the CORE lab at UNIST, enables the coupling of related physics modules. MPCORE can perform both transient and depletion studies, and it can read restart files for transient and multicycle depletion simulations. By utilizing external coupling, the need for internal code modifications has been reduced, and the advantages of modular independence and reusability have been realized. Additionally, the framework includes several important features, such as an adaptive time step algorithm [29], python input and output processing and interpolation to exchange data between modules, based on the different mesh requirements for each module. The parallel implementation of independent modules allows for efficient use of available resources. In this research, fixed burnup steps are used for cycle depletion to facilitate comparison with other codes.

Two types of coupling, one-way and two-way, have been employed for TH and FP. In some instances, researchers have utilized one-way coupling between TH and FP codes, as evidenced by previous studies [30–32]. In this approach, no data is transferred from the FP to the TH code. The coupling between neutronics and TH was first accomplished incrementally. Subsequently, the FP code was added, allowing for

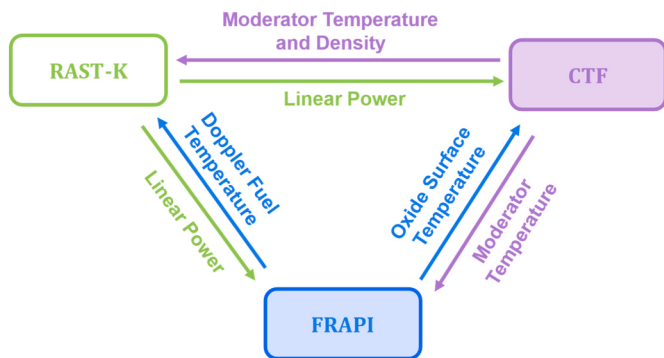


Fig. 2. Two-way coupling between TH and FP modules.

updated fuel temperature information to be provided to the neutronics module. The TH module uses its own fuel thermal conductivity correlations to compute boundary conditions (clad or coolant temperature) for the FP code, while also supplying coolant information to the neutronics module. Fig. 1 depicts the one-way coupling approach between the TH and FP modules.

Certain researchers employ two-way coupling between FP and TH, utilizing the TH module solely for coolant-related parameters [16,33]. With this coupling method, FP is responsible for fuel, gap, and clad thermal conductivity, and provides oxide surface temperature to the TH code. FP codes are optimized for fuel, gap conductivity with burnup, oxide thermal barrier modeling, and are especially useful for multicycle scenarios. In the reshuffling of older fuel assemblies to a fresh core, burnt fuel rod parameters are transferred to FP code by restart files. The TH code does not require the storage of restart information, as it utilizes the oxide surface temperature predicted by the FP code.

Fig. 2 illustrates how two-way coupling is performed between each pair of physics modules. RAST-K provides linear power to both the FRAPI and CTF modules. FRAPI solves for burnup-dependent fuel conduction with dynamic gap heat conductance, providing fuel Doppler temperature to RAST-K and oxide temperature to CTF. CTF, in turn, supplies coolant temperature and density to RAST-K, and coolant temperature to FRAPI.

The Picard convergence method is employed at each burnup step for the values of various parameters, such as critical boron concentration (CBC), linear power, fuel-clad-moderator temperatures, moderator density, and film heat transfer coefficients. Fig. 3 illustrates the overall flow scheme for the MPCORE system. At the outset of the program, a python script is used to generate input files for all modules. C++ module of MPCORE read in any necessary restart files containing burnup information, number densities, and gap conductance from the previous cycle.

RAST-K is responsible for solving flux and power distribution, providing this distribution to FRAPI. FRAPI, in turn, solves fuel heat conduction and provides oxide surface temperature to CTF in two-way coupling. CTF then solves for heat transfer from the oxide layer to the coolant in two-way coupling. In one-way coupling, however, FRAPI does not provide oxide temperature information to CTF, and CTF employs its own conduction solver to determine coolant temperature.

### 4. Model description

Benchmark documents [1,21] include nuclear fuel depletion data for three cycles of the Watts Bar reactor. The benchmark results were obtained using a variety of standalone and Multiphysics codes. In computational codes, reproducing the power history of an actual power plant can be challenging. To address this issue, the benchmark team [21] has provided an appropriate power history that can be utilized to accurately model the depletion cycle. The Watts bar reactor comprises of 193 Westinghouse designed 17 x 17 assemblies, each containing 264

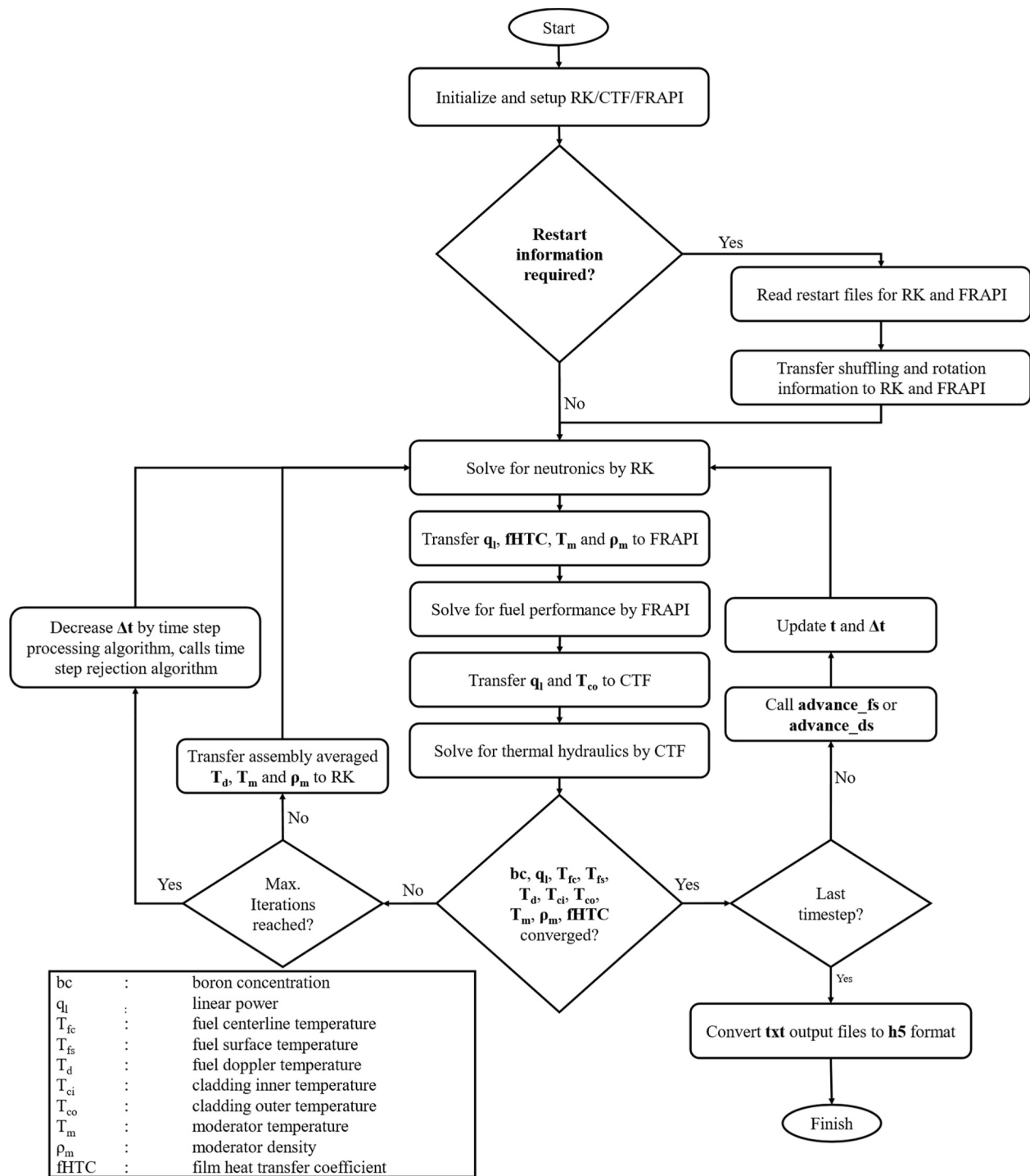


Fig. 3. Flow scheme of MPCORE.

fuel rods and 25 instrumentation/guide tubes. For this study, a quarter core with 56 assemblies is modeled.

#### 4.1. Modeling details

In MPCORE, the Multiphysics modules can have different axial meshes. One of them is the requirement of different axial meshing for spacer grid and non-spacer grid cross-section in the NK code. RAST-K calculation is conducted using a three-dimensional quarter-core model with four nodes for each assembly and 54 axial nodes. Equilibrium xenon calculations and CBC searches are conducted at each burnup

point. FRAPI and CTF use 24 axial meshes, and data transfer between the codes is interpolated by MPCORE. The FP module uses five radial meshes for the fuel region and three radial meshes for the cladding region. FRAPI uses a dynamic gap conductance model, which is particularly important for multicycle scenarios, where burnt fuel has high conductance from the start, while fresh fuel has low conductance.

#### 4.2. Model verification

Rotation and shuffling in multicycle depletion scenarios have been implemented in MPCORE and verified for cycle 2 and cycle 3 of Watts

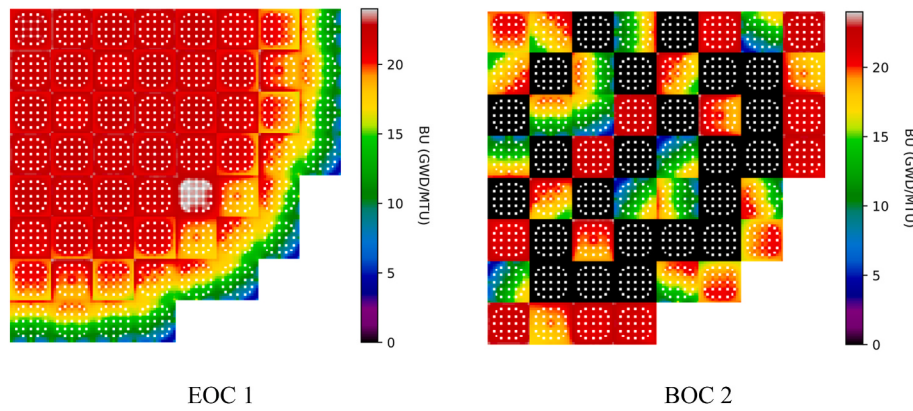


**Fig. 4.** EOC 1 and BOC 2 axial integrated burnup information from FRAPCON-MPCORE.

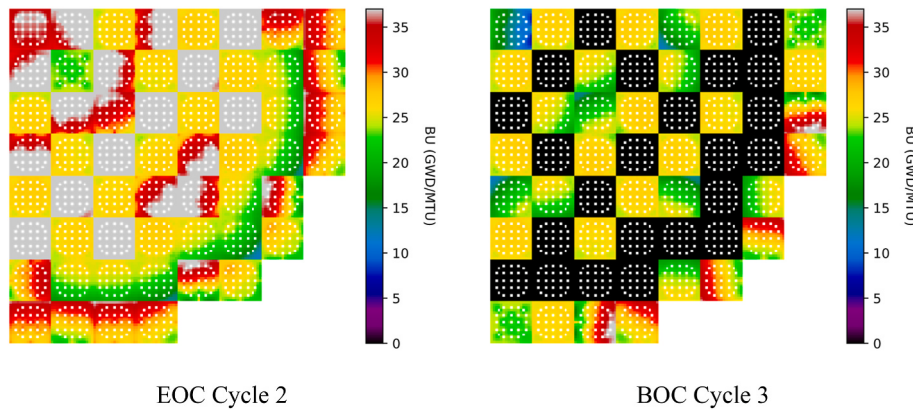


**Fig. 5.** EOC 2 and BOC 3 axial integrated burnup information from FRAPCON-MPCORE.

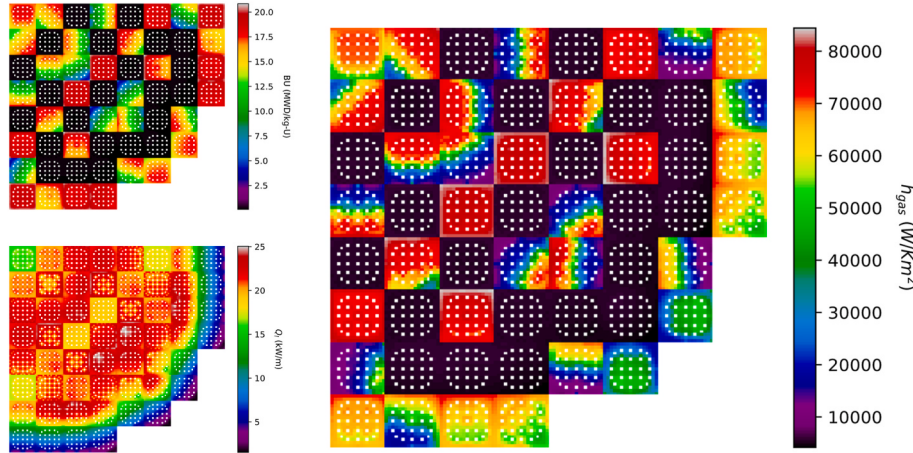


**Fig. 6.** Gap conductivity as a function of burnup and linear power at 3.7 EFPD cycle 2.

bar reactor. Burnup information at the end of cycle (EOC) 1 and beginning of cycle (BOC) 2 is given in Fig. 4.

Similarly, EOC 2 and BOC 3 burnup information is given in Fig. 5. FRAPCON axial integrated burnup information is compared for three cycles to verify the shuffling and rotation capability of MPCORE.

MPCORE now includes shuffling and rotation capability for RAST-K and FRAPCON. To further validate the accuracy of the model, it is necessary to verify the value of gap conductance as a function of burnup and power. It is observed that the gap width reduces with burnup, leading to an increase in gap conductance. Conversely, fuel conductivity

decreases with burnup. Fig. 6 provides the axial integrated burnup and linear power for cycle 2 at 3.7 effective full power days (EFPD), along with the axial integrated gap conductivity values.

Similarly, gap conductivity with burnup and power is given for cycle 3 at 5.1 EFPD in Fig. 7.

It is worth noting that FRAPCON can model conductance through IFBA-coated fuel pins, which give rise to higher internal gas pressure on burnup. In the second and third cycles of the Watts Bar reactor, some fuel rods have IFBA coating, which reduces the gap width at BOC. Detailed modeling is performed in FRAPCON, with information on gap

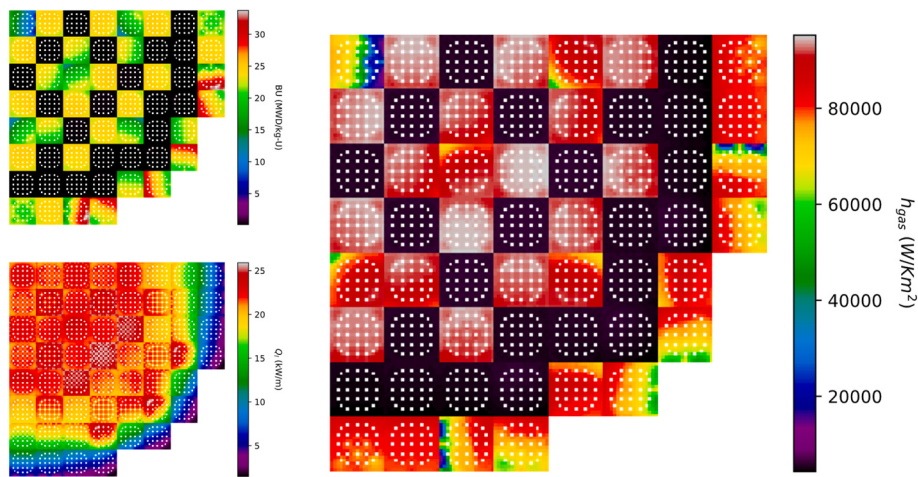


**Fig. 7.** Gap conductivity as a function of burnup and linear power at 5.1 EFPD cycle 3.

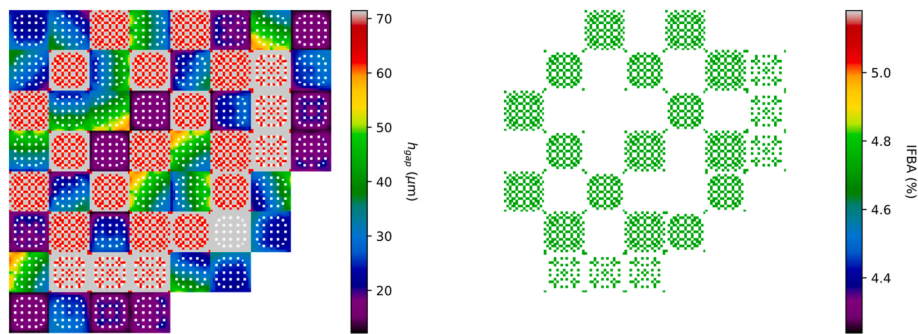


**Fig. 8.** Gap width and IFBA % for each rod in FRAPCON BOC 2.

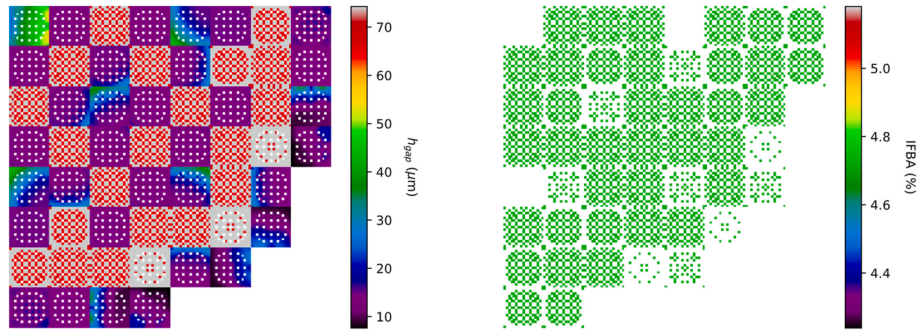


**Fig. 9.** Gap width and IFBA % for each rod in FRAPCON BOC 3.

thickness and IFBA relative percentage provided in a Fig. 8. The IFBA layer outside the fuel is considered to provide oxide surface temperature in two-way coupling, while one-way coupling relies on CTF's own fuel conduction to calculate the coolant temperature, whereas CTF cannot model IFBA coated pins.

Cycle 3 also includes IFBA pins in certain assemblies that are accurately simulated using python input scripting of MPCORE. Fig. 9 displays the gap thickness and IFBA relative percentage at the center height of the core at the BOC 3. Furthermore, the gap thickness of the spent fuel is adjusted using restart files.

## 5. Results

Depletion analysis of the Watts Bar reactor for three cycles is conducted using the MPCORE framework. Reference results for the first

cycle are obtained using the MCS/TH1D [34]. The Monte Carlo results for NK parameters are in close agreement with the measured results, and thus the NK parameters of MPCORE are compared with MCS/TH1D results. According to previous study [35], fuel thermal conductivity decreases with increasing burnup, while gap conductivity increases due to gap closure. Thus, these two effects cancel each other and the difference in coolant temperature should not be significant between one-way and two-way coupling. However, coolant temperature is still higher in one-way coupling due to the high fuel thermal conductivity in CTF. FRAPCON considers burnup-dependent conduction correlations and uses restart files for cycle 2 and cycle 3. On the other hand, CTF does not have a restart file and considers each fuel assembly as fresh fuel unless burnup information is provided. CTF also assumes the same fuel and gap parameters for all fuel rods in an assembly, while FRAPCON allows for different gap widths in each axial mesh of fuel rod. In

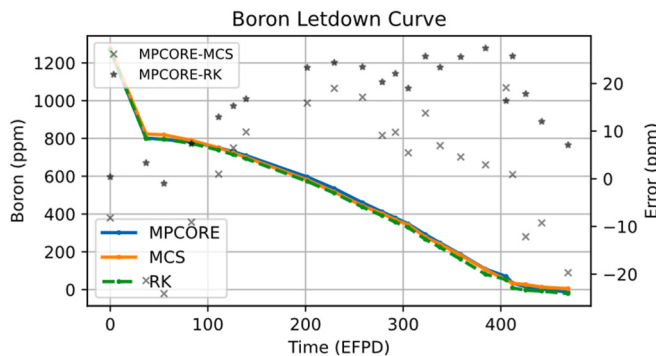


**Fig. 10.** Boron concentration with time cycle 1.

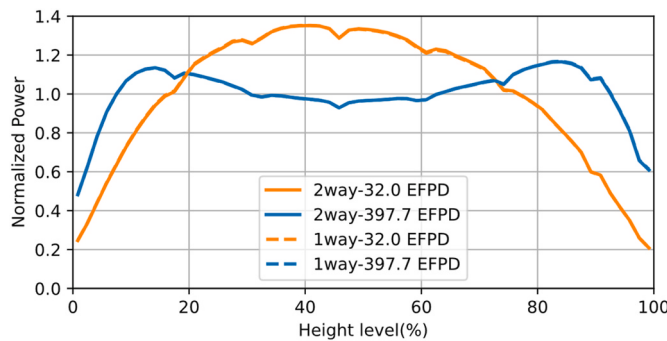


**Fig. 11.** Normalized power profile at 32 EFPD and 397.7 EFPD

addition, IFBA coating and hollow fuel rods can be modeled in FRAPCON.

### 5.1. Cycle 1 results

The results of depletion for Watts Bar cycle 1, with both one-way and two-way coupling, are presented in this study. Additionally, the verification of Boron concentration and power profile for MPCORE was done with MCS/TH1D results in Fig. 10. In this figure, the solid lines are plotted against the left y-axis, representing MPCORE results obtained using two-way coupling, while the legend for the error terms (\*) and (x) corresponds to the right y-axis. Furthermore, the difference between two-way and one-way coupling for NK parameters is minimal for power profile as shown in Fig. 11.

Fig. 12 shows the core average parameter values acquired through both two-way and one-way coupling. The discrepancy between the two values is depicted in green color and presented on the secondary y-axis. The difference was computed as follows:

$$Diff = \delta_{\text{two way}} - \delta_{\text{one way}} \quad (4.1)$$

In this study, it was observed that the coolant temperature calculated by CTF fuel conduction and convection is higher than the two-way coupling coolant temperature. This temperature along with linear power drives the FRAPCON conduction. As the coolant temperature is higher, the oxide surface temperature is also higher. The smaller temperature difference between oxide and coolant results in higher average film heat transfer coefficient (HTC) to compensate for the heat transfer.

CHC is important parameter for fuel analysis and accident scenarios [36]. The Multiphysics coupling analysis was conducted to study the hydrogen uptake by zirconium cladding, and the results were based on the DECAR and CTF coupling [23]. An input was generated for BISON using these results, and therefore, BISON was not utilized in the coupling, but rather relied solely on the coolant temperature predicted by CTF as a boundary condition.

The average CHC in this research indicates that the one-way coupling

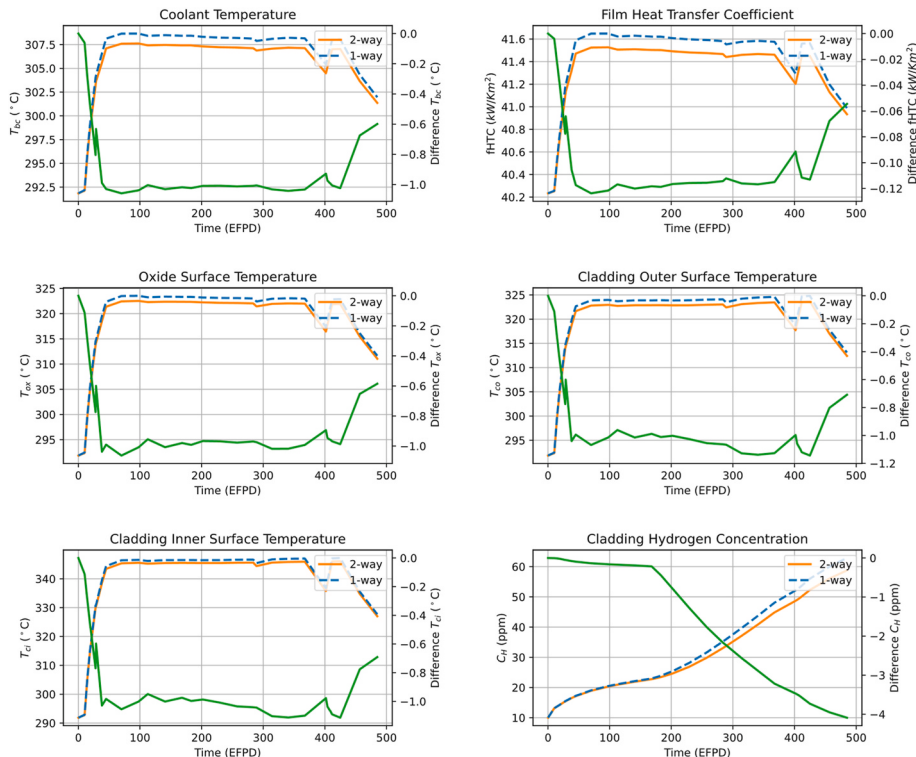


**Fig. 12.** Core averaged parameter value with EFPD for cycle 1.

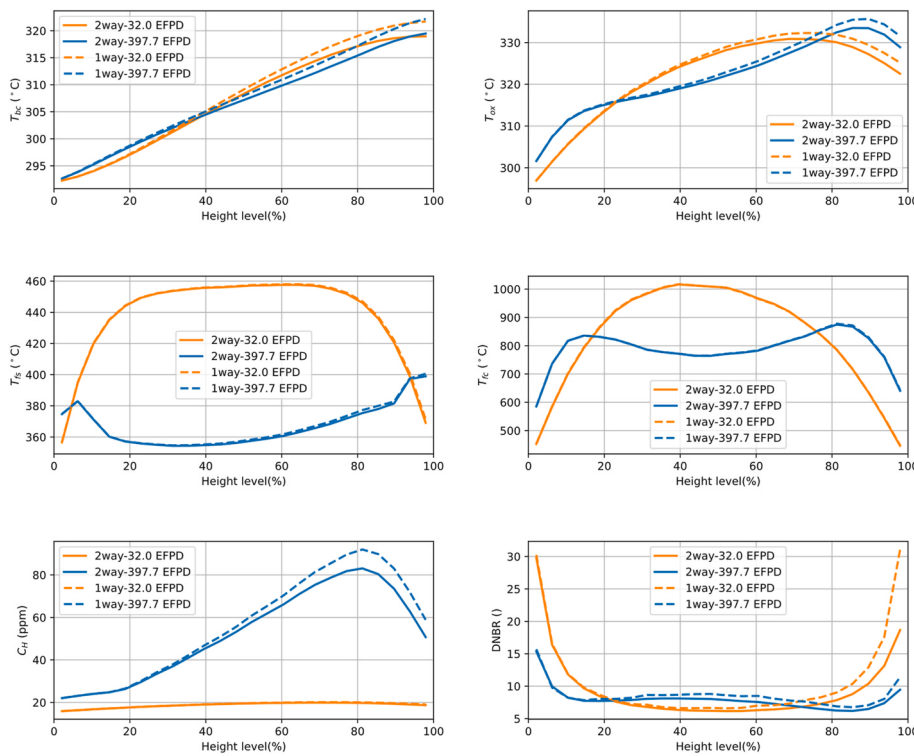


**Fig. 13.** Radial integrated parameter value at 32 EFPD and 397.7 EFPD cycle 1.

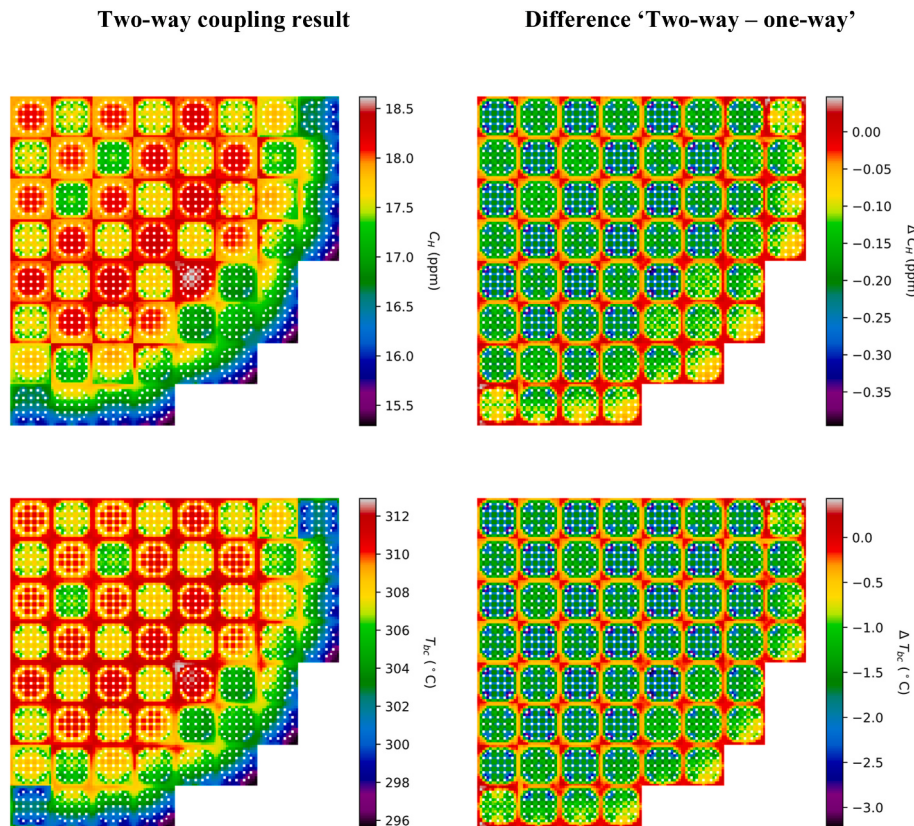
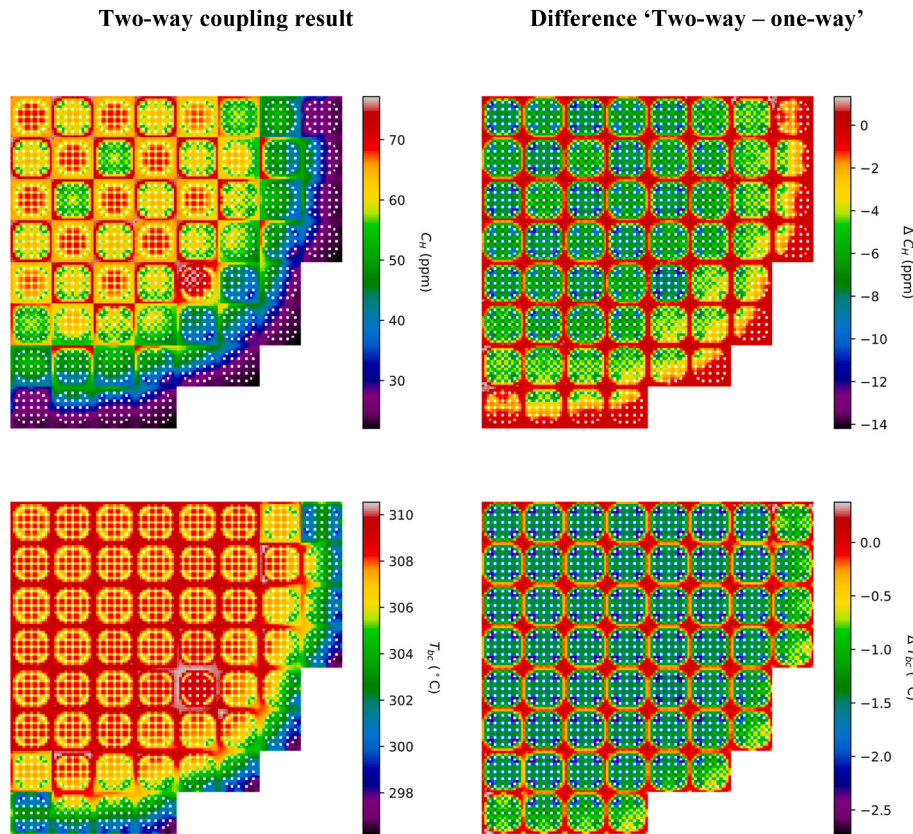


**Fig. 14.** Axial integrated values at 32 EFPD cycle 1.

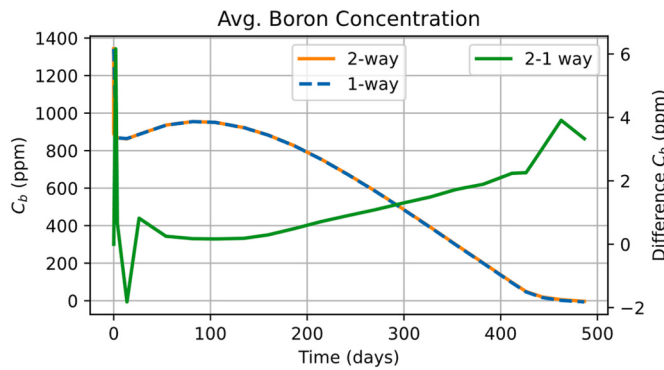
overpredicts the CHC. This difference between one-way and two-way coupling increases with higher burnup.

Fig. 13 displays the axial distribution of core-wise parameters

obtained from both models. The difference between the two coupling approaches is negligible for fuel centerline and fuel surface temperature. This is attributed to the fact that the NK and FP coupling is identical in



**Fig. 15.** Axial integrated values at 397.7 EFPD cycle 1.



**Fig. 16.** Boron concentration with time cycle 2.

both approaches. However, a noticeable difference was observed for the coolant and cladding temperatures, which can have an impact on the DNBR and CHC. At the top axial meshes, due to the sustained high average coolant temperature, the difference in CHC becomes more pronounced.

Fig. 14 illustrates the axial integrated radial values of CHC and bulk coolant temperature obtained from the two-way coupling approach, along with their differences from the one-way approach, at 32 EFPD - the first full power burnup point.

Fig. 15 displays the axial averaged radial parameter values obtained at the final full power stage of 397.7 EFPD. Difference in CHC is higher in the central fuel rods where higher coolant temperature is observed by fuel rods. The average value of gap conductance changes from  $3000 \text{ W/Km}^2$  to  $90000 \text{ W/Km}^2$  (from BOC to EOC) in case of FRAPCON while in CTF it stays in the range of  $5000 \text{ W/Km}^2$  to  $7000 \text{ W/Km}^2$  throughout the cycle. Use of burnup dependent correlation in CTF would have increased

the difference in results.

### 5.2. Cycle 2 results

This section presents the results of the Watts Bar cycle 2 depletion analysis using both one-way and two-way coupling. In cycle 2, certain assemblies contain IFBA pins that are explicitly modeled in FRAPCON. The fresh fuel in cycle 2 has varying enrichment levels in the blanket section of the fuel rods. In two-way coupling, the relevant oxide surface temperatures for these pins are determined based on appropriate fuel conduction. In contrast, the one-way coupling method relies solely on the coolant temperature predicted by CTF. The computed coolant temperature is used as boundary conditions in FRAPCON. Consequently, less boron concentration was required to maintain the criticality state. Section 4.2 verifies the shuffling and rotation capability of MPCORE for Cycle 2, which uses burnt fuel from cycle 1. The gap conductance and burnup are read, and the change in location is identical to the change in core configuration [21]. Fig. 16 illustrates the difference in boron concentration between the two approaches.

Fig. 17 shows the core averaged parameters with burnup for cycle 2. The results indicate that the average CHC is over-predicted by one-way coupling. Moreover, the difference between the two coupling approaches, increases with burnup.

Fig. 18 illustrates the axial distribution of core wise parameters at the first full power burnup point of 3.7 EFPD for both models, as obtained through radial averaging. The parameters near the cladding that are controlled by the FP and TH coupling exhibit a greater difference compared to the parameters near the fuel centerline, which are controlled by the NK and FP coupling.

The radial averaged axial distribution of core wise parameters at last full power stage, 425.7 EFPD, is shown in Fig. 19. The disparity in fuel surface temperature, in two-way coupling, is more pronounced in the top axial mesh due to the lower enrichment in the blanket part of fresh

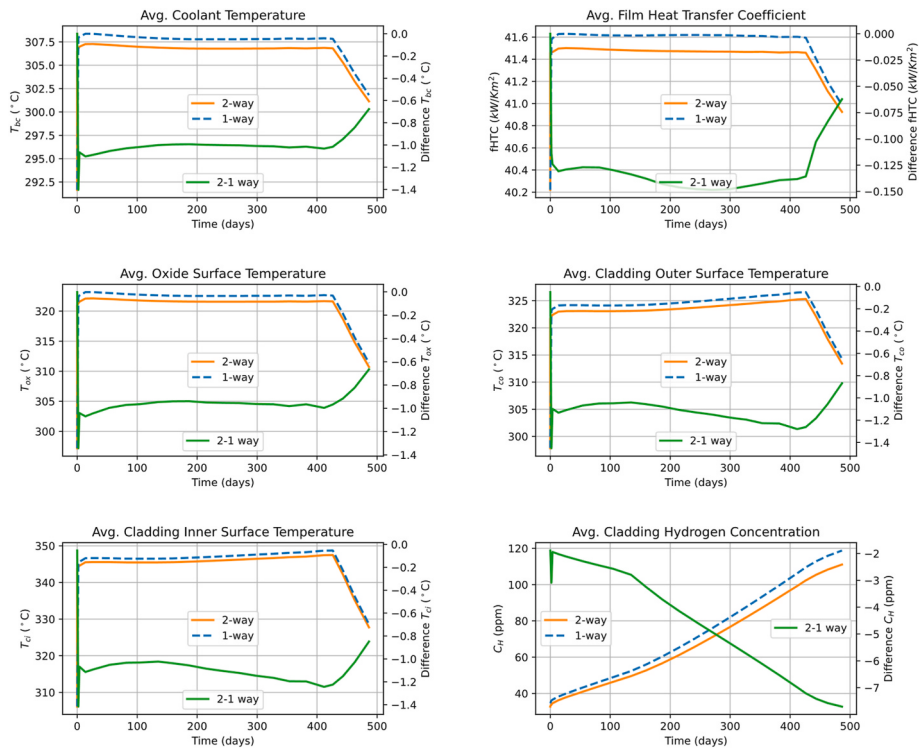


Fig. 17. Core averaged parameter value with EFPD for cycle 2.

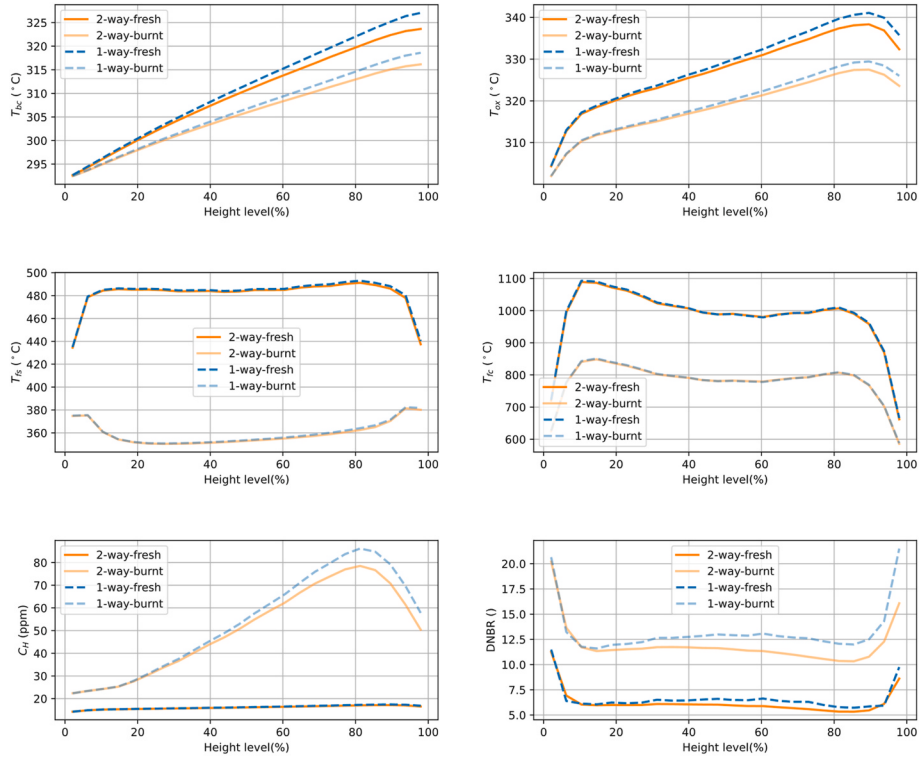


Fig. 18. Radial integrated parameter value at 3.7 EFPD cycle 2.

fuel. When considering the same enrichment, CTF provides a more gradual transition in this area.

The axial integrated coolant temperature and CHC at 3.7 EFPD is shown in Fig. 20. At the start of cycle 2, it is easy to differentiate fresh fuel assemblies from burnt fuel assemblies by checking the CHC

difference.

The axial integrated coolant temperature and CHC at 425.9 EFPD is shown in Fig. 21. The difference in CHC keeps on increasing as the coolant temperature throughout the two cycles is overpredicted in one-way coupling. The average value of gap conductance changes from

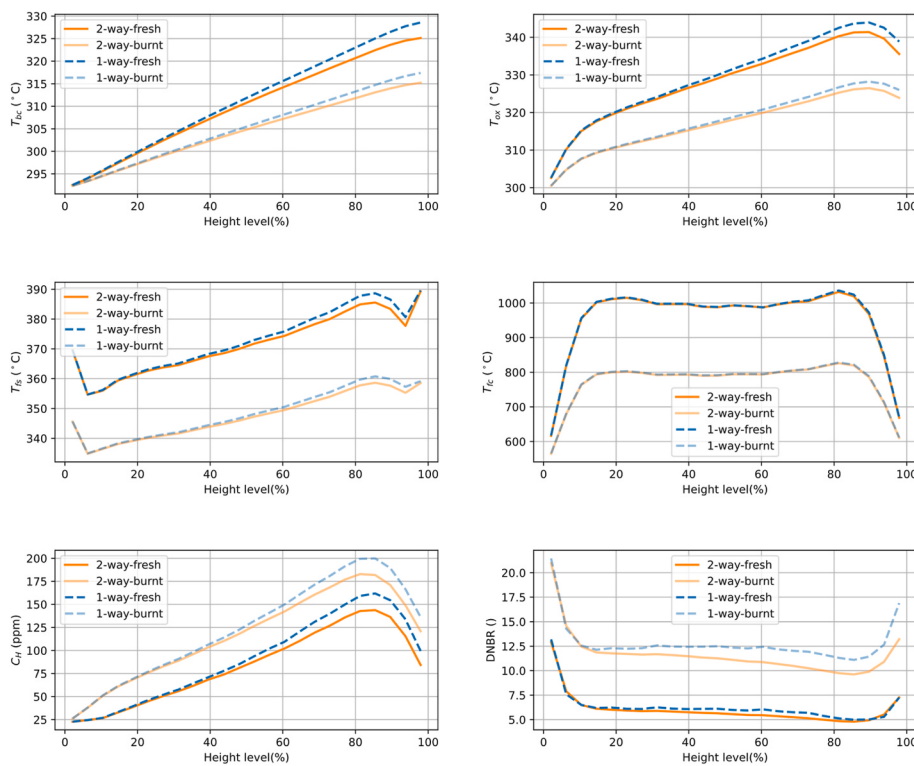


Fig. 19. Radial integrated parameter value at 425.9 EFPD cycle 2.

Two-way coupling result

Difference 'Two-way – one-way'

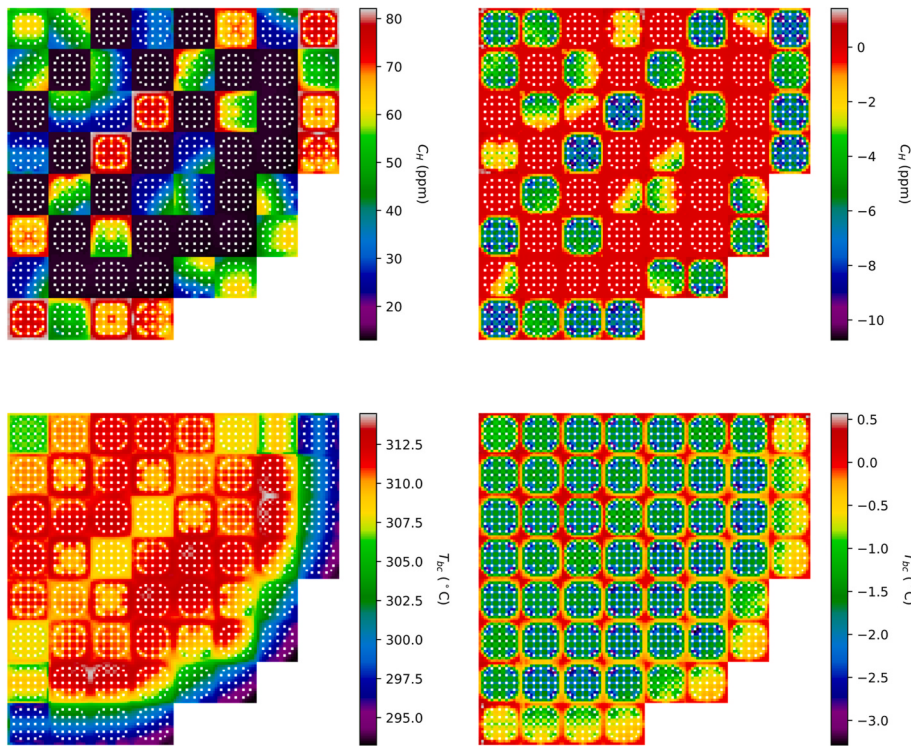


Fig. 20. Axial integrated values at 3.7 EFPD cycle 2.

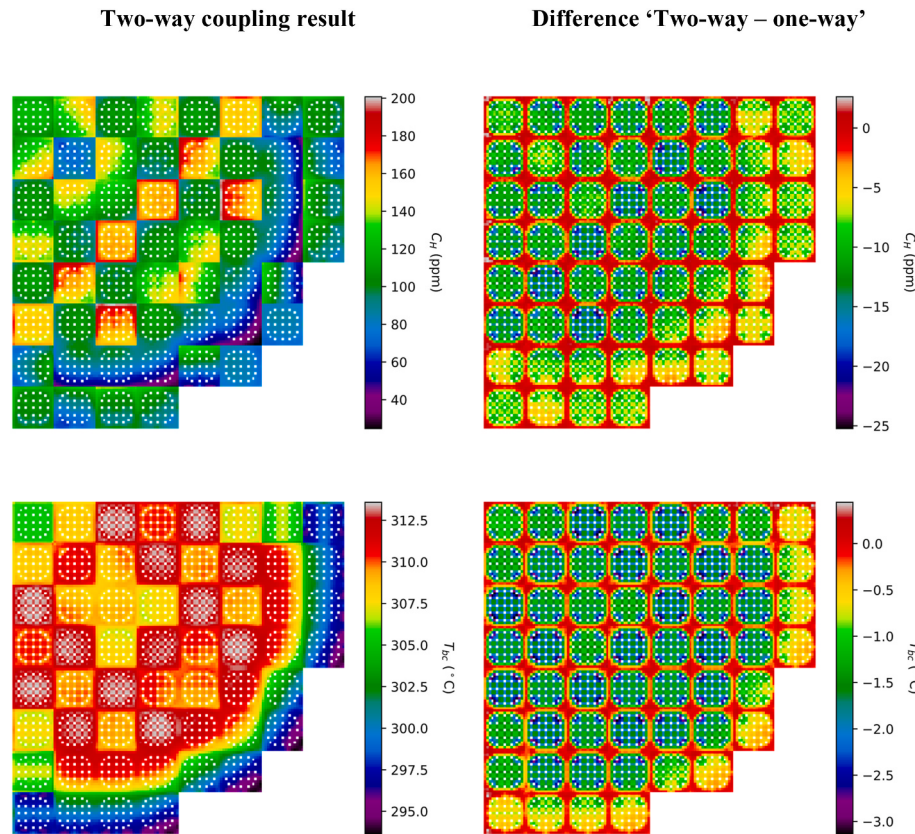


Fig. 21. Axial integrated values at 425.9 EFPD cycle 2.

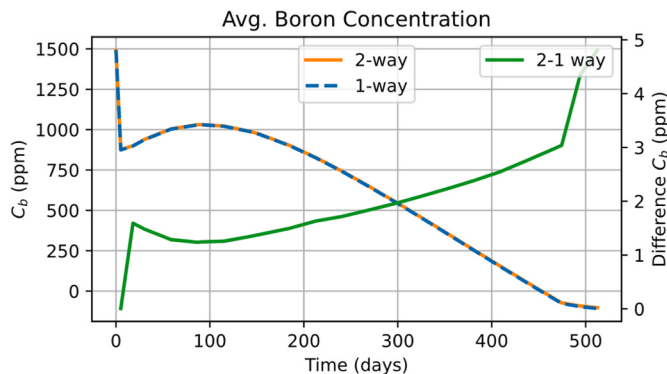


Fig. 22. Boron letdown curve cycle 3.

60000 W/Km<sup>2</sup> to 100,000 W/Km<sup>2</sup> (from BOC to EOC) in case of FRAPCON while in CTF it stays in the range of 5000 W/Km<sup>2</sup> to 7000 W/Km<sup>2</sup> throughout the cycle.

### 5.3. Cycle 3 results

This section presents an analysis of the depletion results for Cycle 3 of the Watts Bar reactor. The analysis includes both one-way and two-way coupling approaches. The fuel assemblies used in Cycle 3 are distinct from those used in Cycle 2, with an even higher enrichment level. Furthermore, Cycle 3 utilizes hollow fuel pins in the blanket fuel region, which initially adds positive reactivity to the core but ultimately removes it by the end of the cycle. This is particularly significant as the beginning-of-cycle (BOC) flux profile peak is at the center, and the top and bottom fuel sections attempt to make it linear. The inner diameter of the hollow fuel is provided to FRAPCON, which can model the fuel heat

conduction for hollow fuel pins. Additionally, the top and bottom hollow fuel pin parts have less enrichment, and the fuel rod modeling in FRAPCON for this cycle requires different axial parameters for selected fuel pins.

The results for one-way and two-way coupling in the MPCORE framework are compared. Section 4.2 verifies the shuffling and rotation capability of MPCORE for Cycle 3, which uses burnt fuel from two different cycles. The gap conductance and burnup are read, and the change in location is identical to the change in core configuration [21]. Furthermore, Fig. 22 shows that the difference in boron concentration for both one-way and two-way modeling increases with burnup.

In this study, the core-averaged parameters were analyzed for the entire cycle duration, and the results are presented in Fig. 23. It was observed that the average gap thickness at EOC 3 was higher than that of EOC 2, resulting in a lower gap heat transfer coefficient for EOC 3 compared to EOC 2. The possible cause for this difference could be attributed to the modeling of hollow fuel pins in the blanket region of the fresh fuel pins. The hollow part provided additional volume for fuel expansion, thereby resulting in an increase in the average core gap width. Additionally, it was found that the average coolant temperature throughout the cycle was higher for one-way coupling, mainly due to the burnup deficient fuel heat conduction modeling in CTF.

The analysis of radial integrated axial core-wise parameters for both models at 5.1 EFPD is presented in Fig. 24. The average values were calculated separately for fresh and burnt fuel to observe their individual effects.

Fig. 25 illustrates a comparison of the axial distribution of core-wise parameters between the two models at 474.4 EFPD. Although the DNBR value for the twice-burnt fuel still exhibits a higher difference, the safety margin is higher with both models, as the proportion of power from burnt fuel is reduced.

The axial integrated radial CHC and coolant temperature for two-way coupling and difference with one-way coupling at 5.1 EFPD is

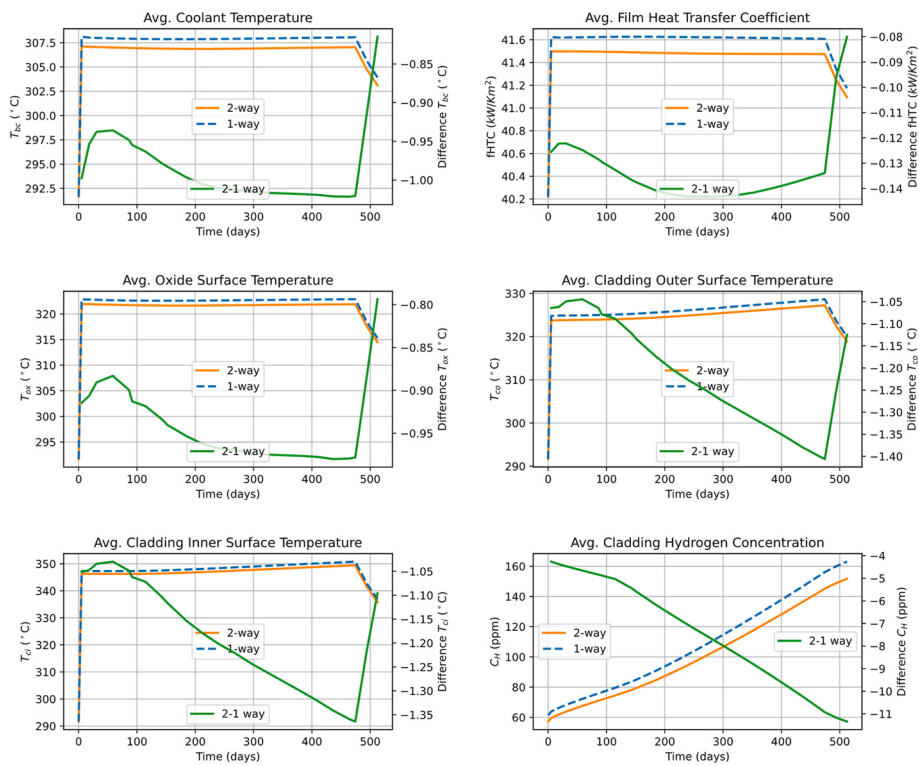


Fig. 23. Parameter average value comparison between one-way and two-way coupling cycle 3.

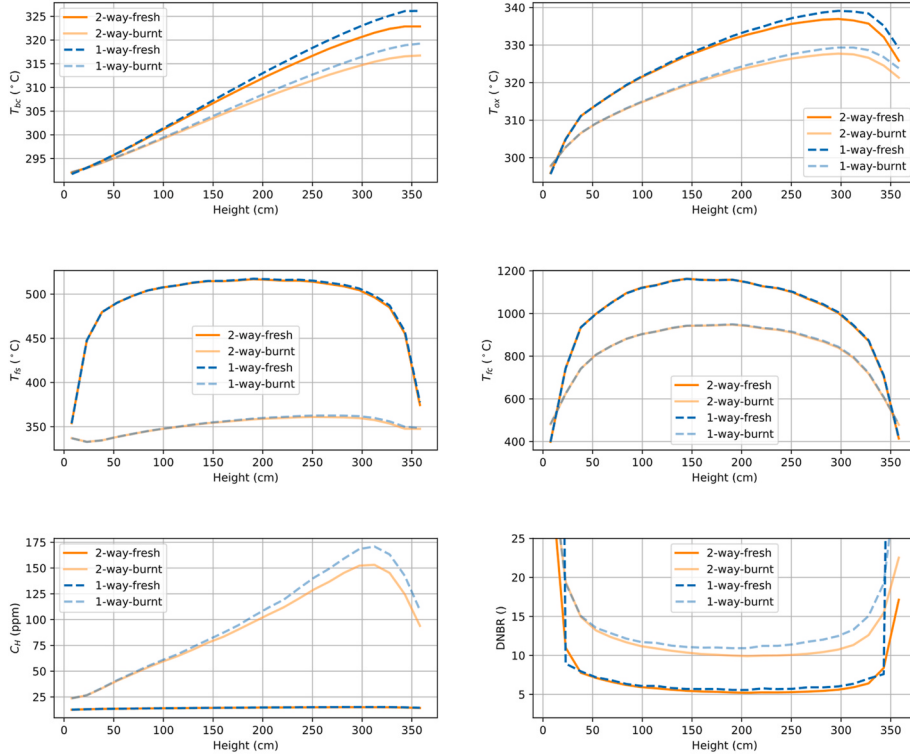


Fig. 24. Radial integrated parameter value at 5.1 EFPD cycle 3.

shown in Fig. 26.

The axial integrated radial CHC and coolant temperature value for two-way coupling and difference with one-way coupling at 474.4 EFPD is shown in Fig. 27. The average value of gap conductance changes from 70000 W/Km<sup>2</sup> to 100,000 W/Km<sup>2</sup> (from BOC to EOC) in case of

FRAPCON while in CTF it stays in the range of 5000 W/Km<sup>2</sup> to 7000 W/Km<sup>2</sup> throughout the cycle.

The results of the 3 cycles have indicated that one-way coupling has resulted in an overestimation of the coolant temperature, leading to an overestimation of the CHC. While simplified models are known to

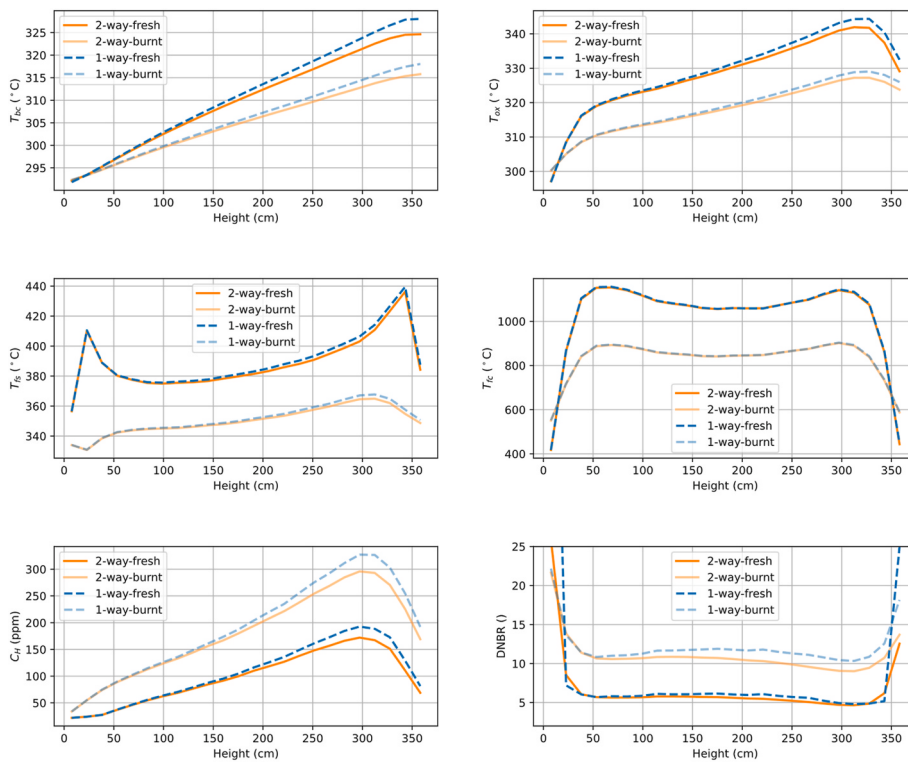


Fig. 25. Radial integrated parameter value at 474.4 EFPD cycle 3.

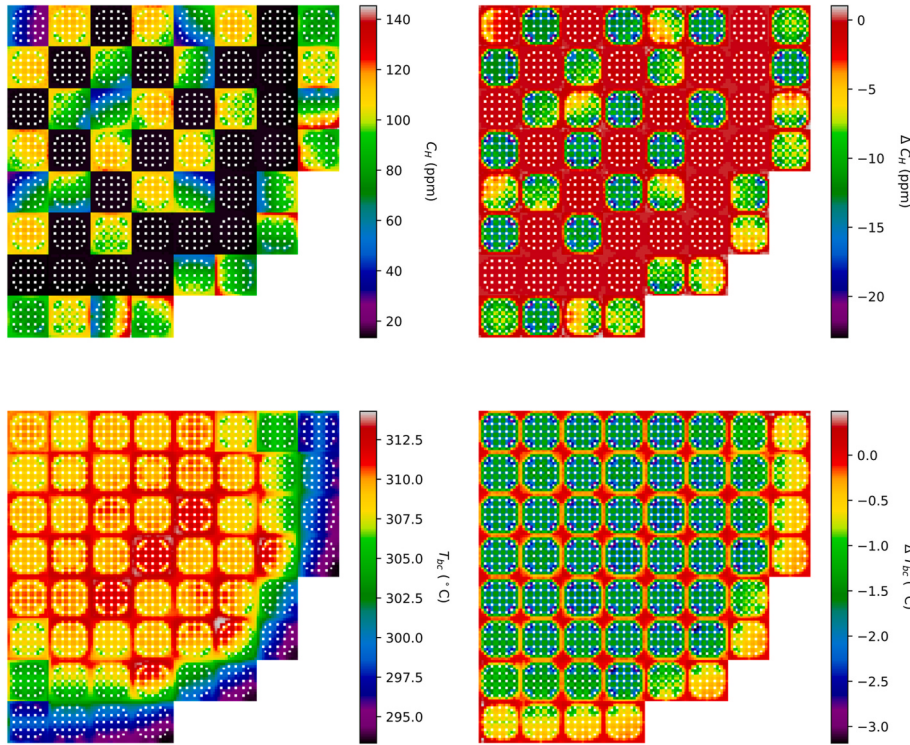
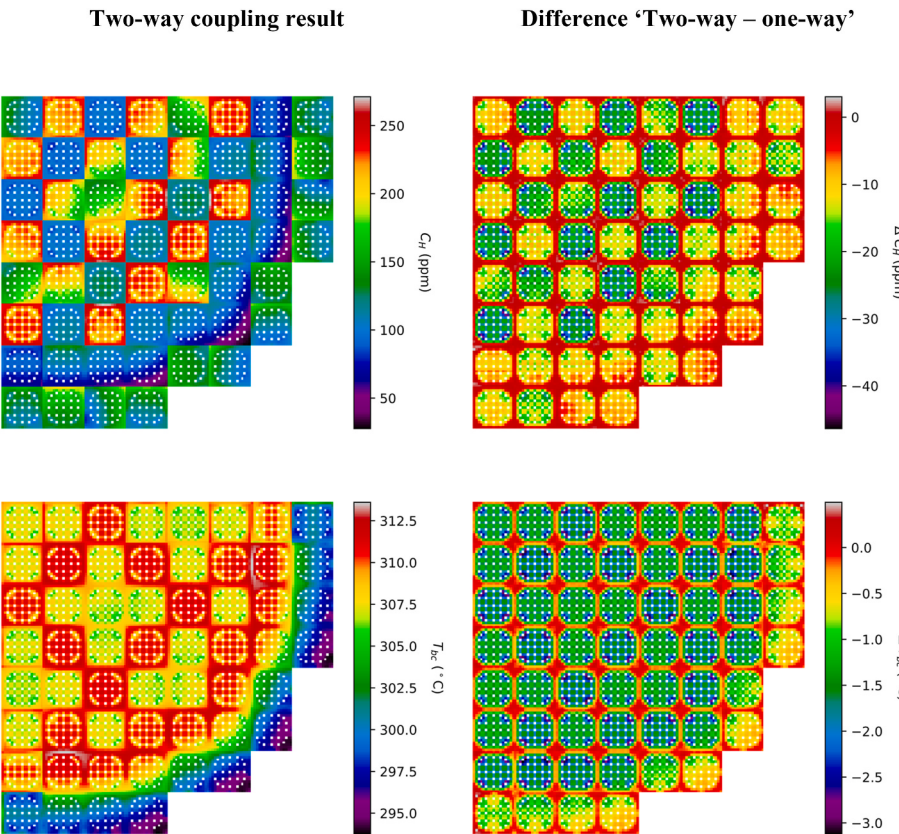
**Two-way coupling result****Difference ‘Two-way – one-way’**

Fig. 26. Axial integrated values at 5.1 EFPD cycle 3.



**Fig. 27.** Axial integrated values at 474.4 EFPD cycle 3.

produce conservative results, accurate results are necessary to avoid overestimating safety parameters. This study has revealed that one-way coupling also overestimates certain safety parameters, as the TH module employs simplified heat conduction correlations. To model safety criteria effectively with respect to FP and cladding properties, appropriate correlations must be used. The conduction option in the TH code is disabled, and the outer surface temperature of the cladding oxide layer is given as a boundary condition for the TH code.

## 6. Conclusion

The study employed the MPCORE framework, which allows for the analysis of multiple physics and cycles, to investigate a multicycle depletion benchmark problem. The framework's shuffling and rotation capabilities were confirmed for three cycles of the Watts Bar reactor. The study used a two-step neutronics code, STREAM/RAST-K, to provide node average power, followed by a pin power reconstruction process. While the MPCORE framework provides values for each pin through its thermal hydraulic and fuel performance modules, RAST-K uses node average values for nodal power.

The study analyzed one-way and two-way coupling strategies of FP and TH codes and conducted a performance comparison for parameters such as cladding hydrogen concentration (CHC), coolant temperature, oxide surface temperature, fuel temperatures, and departure form nucleate boiling ratio (DNBR). Since the coupling of the NK-TH code and NK-FP code was the same in both comparison options, the discrepancy between one-way and two-way coupling for core average parameter values was negligible for power profile, fuel centerline temperature and enthalpy. However, there was a noticeable difference in coolant and cladding temperatures, which can affect DNBR and CHC. At the top axial meshes, the difference in CHC becomes more pronounced, and it increases with higher burnup.

The study found that fine modeling of thermal hydraulic and fuel

performance significantly improved the nodal code's performance. It is worth noting that transport and Monte Carlo-based neutronics code may produce more distinct results with one-way and two-way coupling approaches, as the feedback is applied pin-wise.

## Declaration of competing interest

The authors declare that they have no known competing financial interests or personal relationships that could have appeared to influence the work reported in this paper.

## Acknowledgments

This research was supported by the project (L20S089000) by Korea Hydro and Nuclear Power Co. Ltd. This work was partially supported by Korea Institute of Energy Technology Evaluation and Planning (KETEP) grant funded by the Korea government (MOTIE) [RS-2023-00241302].

## References

- [1] A.T. Godfrey, VERA Core Physics Benchmark Progression Problem Specifications, Oak Ridge National Laboratory, Oak Ridge, 2014. CASL-U-2012-0131-004.
- [2] N. Horelik, et al., Benchmark for Evaluation and Validation of Reactor Simulations, MIT Computational Reactor Physics Group, 2017.
- [3] T. Downar, D. Lee, Y. Xu, T. Kozlowski, PARCS v2.6 U.S. NRC Core Neutronics Simulator Theory Manual, School of Nuclear Engineering, Purdue University, 2004.
- [4] J. Park, et al., RAST-K v2—three-dimensional nodal diffusion code for pressurized water reactor core analysis, Energies 13 (23) (2020).
- [5] J. Choe, et al., Verification and validation of STREAM/RAST-K for PWR analysis, Nucl. Eng. Technol. (2018), <https://doi.org/10.1016/j.net.2018.10.004>.
- [6] J. Jang, et al., Analysis of rostov-II benchmark using conventional two-step code systems, Energies 15 (9) (2022), <https://doi.org/10.3390/en15093318>.
- [7] J. Rhodes, K. Smith, D. Lee, CASMO-5 development and applications, in: Presented at the PHYSOR-2006, Canada, Vancouver, BC, 2006. September 10-14.
- [8] S. Choi, D. Lee, Three-dimensional method of characteristics/diamond-difference transport analysis method in STREAM for whole-core neutron transport

- calculation, *Comput. Phys. Commun.* 260 (2021), <https://doi.org/10.1016/j.cpc.2020.107332>.
- [9] H.J. Park, S.J. Kim, H. Kwon, J.Y. Cho, BEAVRS benchmark analyses by DeCART stand-alone calculations and comparison with DeCART/MATRA multi-physics coupling calculations, *Nucl. Eng. Technol.* 52 (9) (2020) 1896–1906.
- [10] H. Lee, et al., MCS – a Monte Carlo particle transport code for large-scale power reactor analysis, *Ann. Nucl. Energy* 139 (2020), <https://doi.org/10.1016/j.anucene.2019.107276>.
- [11] M. García, J. Leppänen, V. Sanchez-Espinoza, A Collision-based Domain Decomposition scheme for large-scale depletion with the Serpent 2 Monte Carlo code, *Ann. Nucl. Energy* 152 (2021), 108026.
- [12] P.K. Romano, N.E. Horelik, B.R. Herman, A.G. Nelson, B. Forget, K. Smith, OpenMC: a state-of-the-art Monte Carlo code for research and development, *Ann. Nucl. Energy* 82 (2015) 90–97.
- [13] H.-J. Shim, B.-S. Han, J.-S. Jung, H.-J. Park, C.-H. Kim, McCARD: Monte Carlo code for advanced reactor design and analysis, *Nucl. Eng. Technol.* 44 (2) (2012) 161–176.
- [14] M. Vazquez, H. Tsige-Tamirat, L. Ammirabile, F. Martin-Fuertes, Coupled neutronics thermal-hydraulics analysis using Monte Carlo and sub-channel codes, *Nucl. Eng. Des.* 250 (2012) 403–411.
- [15] D.J. Kelly, A.E. Kelly, B.N. Aviles, A.T. Godfrey, R.K. Salko, B.S. Collins, MC21/CTF and VERA multiphysics solutions to VERA core physics benchmark progression problems 6 and 7, *Nucl. Eng. Technol.* 49 (6) (2017) 1326–1338.
- [16] M. García, et al., A Serpent2-SUBCHANFLOW-TRANSURANUS coupling for pin-by-pin depletion calculations in Light Water Reactors, *Ann. Nucl. Energy* 139 (2020), 107213 [Online]. Available: <https://www.sciencedirect.com/science/article/pii/S0306454919307236?via%3Dihub>.
- [17] Z. Liu, B. Wang, M. Zhang, X. Zhou, L. Cao, H. Wu, An internal parallel coupling method based on NECP-X and CTF and analysis of the impact of thermal-hydraulic model to the high-fidelity calculations, *Ann. Nucl. Energy* 146 (2020), 107645 [Online]. Available: <https://www.sciencedirect.com/science/article/pii/S0306454920303431>.
- [18] K.T. Clarno, et al., Coupled neutronics thermal-hydraulic solution of a full-core PWR using VERA-CS, United States, in: Presented at the Conference: PHYSOR 2014, Kyoto, Japan, 2014, pp. 20140928–20141003 [Online]. Available: <https://www.osti.gov/biblio/1154814>.
- [19] Y.S. Jung, C.B. Shim, C.H. Lim, H.G. Joo, Practical numerical reactor employing direct whole core neutron transport and subchannel thermal/hydraulic solvers, *Ann. Nucl. Energy* 62 (2013) 357–374 [Online]. Available: <https://www.sciencedirect.com/science/article/pii/S0306454913003344#f0090>.
- [20] G.K. Delipei, P. Rouxelin, A. Abarca, J. Hou, M. Avramova, K. Ivanov, CTF-PARCS core multi-physics computational framework for efficient LWR steady-state, depletion and transient uncertainty quantification, *Energies* 15 (14) (2022) 5226 [Online]. Available: <https://www.mdpi.com/1996-1073/15/14/5226>.
- [21] S. Stimpson, et al., Pellet-clad mechanical interaction screening using VERA applied to Watts Bar Unit 1, Cycles 1–3, *Nucl. Eng. Des.* 327 (2018) 172–186.
- [22] S. Suman, Influence of hydrogen concentration on burst parameters of Zircaloy-4 cladding tube under simulated loss-of-coolant accident, *Nucl. Eng. Technol.* 52 (9) (2020) 2047–2053.
- [23] I. Davis, O. Courty, M. Avramova, A. Motta, High-fidelity multi-physics coupling for determination of hydride distribution in Zr-4 cladding, *Ann. Nucl. Energy* 110 (2017) 475–485.
- [24] M. Mankosa, M. Avramova, Three-dimensional multi-physics modeling of hydrogen and hydride distribution in zirconium alloy cladding, *Prog. Nucl. Energy* 105 (2018) 294–300.
- [25] R.K. Salko, M.N. Avramova, CTF Pre-processor User's Manual, The Pennsylvania State University, 2016.
- [26] A. Cherezov, H. Kim, J. Park, D. Lee, Fuel rod analysis programming interface for loosely coupled multiphysics system, in: Presented at the in Proceedings of the American Nuclear Society Annual Meeting, Chicago, IL, USA, 2020, 16–19 November.
- [27] K. Geelhood, W. Luscher, P. Raynaud, I. Porter, FRAPCON-4.0: A Computer Code for the Calculation of Steady-State, Thermal-Mechanical Behavior of Oxide Fuel Rods for High Burnup, vol. 1, Pacific Northwest National Laboratory, PNNL, 2015, 19418.
- [28] K. Geelhood, W. Luscher, J. Cuta, I. Porter, in: FRAPTRAN-2.0: A Computer Code for the Transient Analysis of Oxide Fuel Rods vol. 1, Pacific Northwest National Laboratory, PNNL, 2016, 19400.
- [29] A. Cherezov, J. Park, H. Kim, J. Choe, D. Lee, A multi-physics adaptive time step coupling algorithm for light-water reactor core transient and accident simulation, *Energies* 13 (23) (2020), <https://doi.org/10.3390/en13236374>.
- [30] S. Stimpson, et al., Coupled fuel performance calculations in VERA and demonstration on Watts Bar unit 1, cycle 1, *Ann. Nucl. Energy* 145 (2020), 107554 [Online]. Available: <https://www.sciencedirect.com/science/article/pii/S0306454920302528>.
- [31] J. Yu, H. Lee, M. Lemaire, H. Kim, P. Zhang, D. Lee, MCS based neutronics/thermal-hydraulics/fuel-performance coupling with CTF and FRAPCON, *Comput. Phys. Commun.* 238 (2019) 1–18.
- [32] X. Xu, Z. Liu, H. Wu, L. Cao, Neutronics/thermal-hydraulics/fuel-performance coupling for light water reactors and its application to accident tolerant fuel, *Ann. Nucl. Energy* 166 (2022), 108809 [Online]. Available: <https://www.sciencedirect.com/science/article/pii/S0306454921006861>.
- [33] M.I. Radaideh, T. Kozlowski, Combining simulations and data with deep learning and uncertainty quantification for advanced energy modeling, *Int. J. Energy Res.* 43 (14) (2019) 7866–7890, <https://doi.org/10.1002/er.4698>.
- [34] T.D.C. Nguyen, H. Lee, S. Choi, D. Lee, MCS/TH1D analysis of VERA whole-core multi-cycle depletion problems, *Ann. Nucl. Energy* 139 (2020), <https://doi.org/10.1016/j.anucene.2019.107271>.
- [35] B. Roostaii, H. Kazeminejad, S. Khakshournia, Including high burnup structure effect in the UO<sub>2</sub> fuel thermal conductivity model, *Prog. Nucl. Energy* 131 (2021), 103561.
- [36] O. Courty, A.T. Motta, J.D. Hales, Modeling and simulation of hydrogen behavior in Zircaloy-4 fuel cladding, *J. Nucl. Mater.* 452 (1–3) (2014) 311–320 [Online]. Available: <https://www.sciencedirect.com/science/article/pii/S0022311514002803>.